

Radiative corrections to $W_L W_L$ scattering in composite Higgs models

Domènec Espriu, Federico Mescia, and Brian Yencho

*Departament d'Estructura i Constituents de la Matèria, Institut de Ciències del Cosmos (ICCUB),
 Universitat de Barcelona, Martí Franquès 1, 08028 Barcelona, Spain*

(Received 15 July 2013; published 3 September 2013)

The scattering of longitudinally polarized electroweak bosons is likely to play an important role in the elucidation of the fundamental nature of the electroweak symmetry breaking sector and in determining the Higgs interactions with this sector. In this paper, by making use of the equivalence theorem, we determine the renormalization properties of the electroweak effective theory parameters in a model with generic Higgs couplings to the W and Z bosons. When the couplings between the Higgs and the electroweak gauge bosons deviate from their Standard Model values, additional counterterms of $O(p^4)$ in the usual chiral counting are required. We also determine in the same approximation the full radiative corrections to the $W_L W_L \rightarrow Z_L Z_L$ process in this type of model. Assuming custodial invariance, all the related processes can be easily derived from this amplitude.

 DOI: [10.1103/PhysRevD.88.055002](https://doi.org/10.1103/PhysRevD.88.055002)

PACS numbers: 12.60.Fr, 12.60.-i

I. INTRODUCTION

Much of the current theoretical work concerning the LHC implications for the electroweak symmetry breaking sector (EWSBS) focuses on the deviations of the Higgs boson couplings to the electroweak gauge sector rather than the self-couplings of the gauge bosons themselves.¹ Yet, any deviations of the former from their Standard Model (SM) values turn out to have implications for the latter; they are intimately intertwined at loop level and should be understood together, as unitarity considerations demand. We seek in the present paper to provide a consistent framework for future studies of both in the scattering of longitudinally polarized electroweak gauge bosons.

In a previous paper [1] we have already examined the implications of unitarity in the scattering of longitudinally polarized electroweak gauge bosons when—in addition to the usual SM Lagrangian with a light scalar state (the Higgs particle with $M_H \simeq 125$ GeV [2,3])—one includes an EWSBS assumed to be strongly interacting. This sector can be described at energies, $M_H^2 < s < (4\pi v)^2$ by an electroweak chiral effective Lagrangian (EChL) [4]. In [1] we included a set of $O(p^4)$ operators to describe the strongly interacting EWSBS but assumed that the couplings between the Higgs and the electroweak gauge bosons were indistinguishable from the values that they take in the SM. The main purpose of the present work is to relax this hypothesis.

A general chiral Lagrangian with a nonlinear realization of the $SU(2)_L \times SU(2)_R$ symmetry up to $O(p^4)$ terms and including a light Higgs is

$$\begin{aligned} \mathcal{L} = & -\frac{1}{2} \text{Tr} W_{\mu\nu} W^{\mu\nu} - \frac{1}{4} \text{Tr} B_{\mu\nu} B^{\mu\nu} + \frac{1}{2} \partial_\mu h \partial^\mu h \\ & - \rho v (\lambda v^2 + \mu^2) - \frac{1}{2} h^2 (\mu^2 + 3v^2 \lambda) \\ & - d_3 (\lambda v) h^3 - d_4 \frac{1}{4} \lambda h^4 + \frac{v^2}{4} \left(1 + 2a \left(\frac{h}{v} \right) \right. \\ & \left. + b \left(\frac{h}{v} \right)^2 \right) \text{Tr} D_\mu U^\dagger D^\mu U + \sum_{i=0}^{13} \mathcal{L}_i + \mathcal{L}_{\text{GF}} + \mathcal{L}_{\text{FP}}. \end{aligned} \quad (1)$$

Here, the U field contains the three Goldstone bosons associated to the breaking of the global group to the custodial subgroup $SU(2)_V$,

$$U = \exp \left(i \frac{w \cdot \tau}{v} \right), \quad (2)$$

the w being the three Goldstone boson fields.² The matrix U transforms as $U \rightarrow LUR^\dagger$ under the action of the global group $SU(2)_L \times SU(2)_R$. The covariant derivative is defined as

$$D_\mu U = \partial_\mu U + \frac{1}{2} i g W_\mu^i \tau^i U - \frac{1}{2} i g' B_\mu^j U \tau^j. \quad (3)$$

The Higgs field h is a gauge and $SU(2)_L \times SU(2)_R$ singlet. The vacuum expectation value $v \simeq 250$ GeV gives the right dimensions to the exponent in U . The terms \mathcal{L}_{GF} and \mathcal{L}_{FP} in Eq. (1) correspond to the gauge-fixing and Faddeev-Popov pieces, respectively, whereas the term

$$\sum_{i=0}^{13} \mathcal{L}_i = \sum_{i=0}^{13} a_i \mathcal{O}_i \quad (4)$$

¹Anomalous four gauge boson couplings have not been measured yet in LHC experiments at the time of writing this paper.

²We shall denote by z the neutral Goldstone boson $w^\pm = (w^1 \mp w^2)/\sqrt{2}$.

includes a complete set of CP -even, local, Lorentz, and gauge invariant operators, four-dimensional operators \mathcal{O}_i constructed with the help of the field U , covariant derivatives, and the $SU(2)_L \times U(1)_Y$ field strengths $W_{\mu\nu}$ and $B_{\mu\nu}$. A complete list can be found in [4] and also in [1]. While we will still restrict ourselves to a small subset of all possible general couplings we study those that are experimentally accessible now or in the near future.

In Eq. (1) we have included with respect to [1] two extra parameters a and b controlling the coupling of the Higgs to the gauge sector. Following conventions in [5], we have also introduced two additional parameters d_3 and d_4 that are commonly used in composite Higgs scenarios. They parametrize the three- and four-point interactions of the Higgs field in an effective way. Needless to say that in a composite Higgs scenario, such as the one we have in mind, the Higgs potential need not be renormalizable and higher powers of the field h could appear. There could be additional interaction terms with the electroweak gauge sector of $O(h^3)$ or higher. None of this should affect the results below.

The SM case corresponds to $a = b = d_3 = d_4 = 1$ in Eq. (1). Current LHC results indicate that a and b are not too far from these SM values [6], but at present, deviations from these SM values cannot be excluded. In [1] we assumed that the extended EWSBS would manifest itself only through the appearance of nonzero values for the a_i $O(p^4)$ coefficients but a and b (as well as d_3 and d_4) were assumed to be very close to 1. This is the most conservative hypothesis. However, even if $a \simeq b \simeq 1$, if the EWSBS is such that $O(p^4)$ operators are present, unitarity violations reappear at large energies in a way apparently similar to what happens in models that were copiously studied in the past [7] in the context of a very heavy Higgs or Higgsless theories.

In [1] we calculated the scattering amplitudes using the longitudinal components of the vector bosons themselves as external states, rather than the corresponding Goldstone bosons³ as it is customarily done when one takes advantage of the equivalence theorem [8]. The reason to do so is that at the energies being now explored at the LHC, corrections to the equivalence theorem can be of some relevance [9].

We enforced unitarity through the use of the inverse amplitude method [10]. We found that, even when including a light SM Higgs boson of mass $M_H = 125$ GeV, the unitarity analysis predicts the appearance of dynamical resonances in much of the parameter space of the higher-order coefficients. Their masses extend from as low as 300 GeV to nearly as high as the cutoff of the method of

$4\pi v \simeq 3$ TeV, with rather narrow widths typically of order 1 to 10 GeV. In the absence of these resonances virtually all parameter space of the anomalous couplings could be excluded. However, we also showed that the actual signal strength of these resonances, when compared with current Higgs search data, was such that they were not currently being probed in LHC Higgs search data. Yet, if anomalous vector boson couplings exist, the resulting dynamical resonances they predict should definitely be observable with future LHC data.

The study in [1] therefore showed that there is a direct connection—also when a light Higgs is present—between anomalous four gauge boson couplings and the underlying structure of dynamical resonances in the scalar and vector channels. This emphasizes the importance of measuring these couplings (currently not yet observed at the LHC) to elucidate the fundamental nature of the EWSBS. These measurements have to go hand in hand with the search for the putative additional resonances, bearing in mind that their peak heights and widths bear little resemblance to the Higgs signal (in the scalar sector) or even to what is expected in previously studied strongly interacting theories (particularly in the vector channel). The reason being that the unitarization of the scattering amplitudes with a light Higgs profoundly changes the resonance structure with respect to the Higgsless (or a very heavy Higgs) scenario in extended scenarios of EWSBS. The situation could be also more intriguing if the hypothesis of setting a and b to their SM values, namely $a = b = 1$, is relaxed as unitarity violations are already apparent at tree level.

Before the phenomenological analysis however, the case $a \neq 1$ and $b \neq 1$ requires a complete new study of the radiative corrections, including a detailed study of the divergences and counterterms in this new scenario. This is part of the present work. We will also present a complete calculation of the one-loop $W_L W_L \rightarrow Z_L Z_L$ scattering amplitude (and by extension, upon use of custodial symmetry, of all four longitudinal electroweak gauge boson couplings). The one-loop calculation will be done by making use of the equivalence theorem [8], where the longitudinal components are replaced by the corresponding Goldstone bosons. This approximation is enough to derive the counterterms relevant for the process being discussed. The calculation is done in the nonlinear realization discussed above, as this is the natural language in composite Higgs models. Note that although S -matrix elements are independent of the particular parametrization, renormalization constants need not be.

Finally we mention that when computing electroweak gauge boson scattering amplitudes by making use of the equivalence theorem approximation, particularly if the calculation is done in the gauge where the Goldstone bosons are massless, some subtleties appearing in a complete calculation are not present. For instance, the

³In [1] we treated the tree-level and the imaginary part of the one loop exactly, but we actually had to resort to the equivalence theorem for the real part of the one-loop correction in order to keep the calculation manageable.

results are automatically custodially invariant as one is assuming $g = g' = 0$. Crossing symmetry is also easily implemented by the usual exchanges of the Mandelstam variables. Therefore it is particularly simple to reproduce all amplitudes from the $ww \rightarrow zz$ one and, accordingly, only higher-dimensional operators that are manifestly custodially invariant are needed when moving away from the SM. However, in a full calculation of the $W_L W_L \rightarrow Z_L Z_L$ amplitude, including $O(g, g')$ corrections, new non-custodially invariant operators would be required as counterterms. Furthermore, crossing symmetry (although obviously still holding) is harder to implement (see e.g. the discussion in [1]). We emphasize once more that none of

this affects the determination of the counterterms derived in this paper.

II. LAGRANGIAN AND COUNTERTERMS

The Lagrangian in Eq. (1) will be our starting point. The parameters there have to be considered as renormalized quantities. We trade μ for M_H^2 using $M_H^2 \equiv (\mu^2 + 3v^2\lambda)$. We will use a renormalization scheme where the relation $M_H^2 = 2\lambda v^2$ that holds true at tree level remains true for renormalized quantities.

Next we have to consider the counterterm Lagrangian. This will be

$$\begin{aligned} \delta\mathcal{L} = & -hv(\delta M_H^2 - 2v^2\delta\lambda - 2\lambda\delta v^2) - \frac{1}{2}\delta M_H^2 h^2 - d_3\left(\delta\lambda v + \frac{1}{2}\lambda v \frac{\delta v^2}{v^2}\right)h^3 - d_4\frac{1}{4}\delta\lambda h^4 + \left(2\left(\delta a - \frac{1}{2}a \frac{\delta v^2}{v^2}\right)\left(\frac{h}{v}\right)\right. \\ & + \left.\left(\delta b - b \frac{\delta v^2}{v^2}\right)\left(\frac{h}{v}\right)^2\right)\left(\frac{v^2}{4}\text{Tr}D_\mu U^\dagger D^\mu U\right) + \left(1 + 2a\left(\frac{h}{v}\right) + b\left(\frac{h}{v}\right)^2\right)\left(\frac{v^2}{4}\text{Tr}D_\mu U^\dagger D^\mu U\right)_{\delta v^2} \\ & + \delta a_4(\text{Tr}(V^\mu V^\nu))^2 + \delta a_5(\text{Tr}(V^\mu V_\mu))^2. \end{aligned} \quad (5)$$

We have included the possible higher-order terms from the two $O(p^4)$ operators that are relevant for $W_L W_L$ scattering in the custodial limit, namely \mathcal{L}_4 and \mathcal{L}_5 (see e.g. [1] for details). We omit the pieces that are not relevant for $W_L W_L$ scattering. In the treatment of this paper noncustodial $O(p^4)$ operators are not needed.

The counterterm Lagrangian needs some explanation. To begin with, we have not introduced counterterms for d_3 and d_4 as they affect mostly the renormalization of the Higgs self-interactions of which there is no experimental information at present. Their renormalization should not affect the counterterms that interest us most, namely those directly related to $W_L W_L$ scattering, such as δa_4 and δa_5 . Secondly, there are additional δv^2 counterterms coming from the third line of Eq. (5) that depend on the number of factors of v in the different terms of the U expansion. For instance, terms like

$$\frac{1}{2}\partial_\mu z \partial^\mu z + \partial_\mu w^+ \partial^\mu w^- \quad (6)$$

will have no corresponding counterterm because they contain no factor of v . On the other hand, terms with more than two w fields will result in counterterms. For example, consider one term contributing to the four-point interaction

$$\begin{aligned} & \left(\frac{1}{3v^2}\right)z\partial_\mu z(\partial^\mu w^+ w^- + \partial^\mu w^- w^+) \\ & \rightarrow -\left(\frac{\delta v^2}{v^2}\right)\left(\frac{1}{3v^2}\right)z\partial_\mu z(\partial^\mu w^+ w^- + \partial^\mu w^- w^+). \end{aligned} \quad (7)$$

In addition there are wave-function renormalization constants for the Higgs field, Z_H , and for the Goldstone boson fields, Z_w . Note that there is no mass term (and no corresponding counterterm) for the Goldstone bosons as we shall consistently work in the 't Hooft-Landau gauge, where Goldstone bosons are strictly massless. The renormalization conditions we will employ are that (i) the tadpoles vanish at one loop, (ii) the mass parameters are the on-shell masses, (iii) and that the relation $\lambda = M_H^2/(2v^2)$ is now true of the renormalized quantities, rather than the bare ones. We also note that condition (ii) only ends up affecting the Higgs mass counterterm, as the Goldstone bosons will remain massless independent of any corrections to the two-point function.

As indicated in the Introduction we shall make use of the equivalence theorem to determine the counterterms and the $W_L W_L$ scattering amplitude rather than using the actual gauge degrees of freedom. As far as the counterterms are concerned, this procedure is good enough to give the correct renormalization of the parameters a , b , a_4 , and a_5 that parametrize the EWSBS and thus the departures from the SM result. As for the finite pieces of the amplitude, the use of the equivalence theorem is just an approximation⁴ that becomes better for $s \gg M_W$. A complete calculation using the gauge degrees of freedom is just too complicated for the present purposes and it is available numerically only for the SM [11].

⁴In [1] we used the equivalence theorem in the 't Hooft-Landau gauge to compute the one-loop real part of the amplitude for simplicity. It was seen there that in spite of this approximation unitarity was approximately preserved.

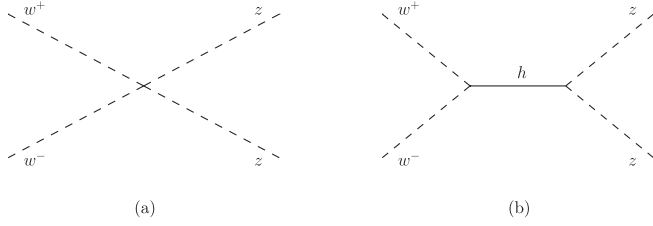


FIG. 1. Tree-level diagrams contributing to the amplitude $w^+ w^- \rightarrow zz$, $i\mathcal{M}_{\text{tree}}$. (a) Contribution to $i\mathcal{M}_{\text{tree}}^a$. (b) Contribution to $i\mathcal{M}_{\text{tree}}^b$.

III. TREE-LEVEL CALCULATION OF $w^+ w^- \rightarrow zz$

The tree-level calculation is fairly straightforward and comes from the sum of the two diagrams as in the usual linear realization case, albeit with different couplings: the $wwzz$ four-point diagram, and the s -channel Higgs exchange diagram. These diagrams are shown in Fig. 1. Their respective contributions are

$$i\mathcal{M}_{\text{tree}}^{(a)} = i\left(\frac{s}{v^2}\right), \quad \text{and} \quad i\mathcal{M}_{\text{tree}}^{(b)} = -i\left(\frac{a^2 s}{v^2}\right)\left(\frac{s}{s - M_H^2}\right). \quad (8)$$

Combined they give

$$i\mathcal{M}_{\text{tree}} = -i\left(\frac{s}{v^2}\right)\left(\frac{(a^2 - 1)s + M_H^2}{s - M_H^2}\right), \quad (9)$$

which obviously reduces to the same value as the linear case for the SM ($a = 1$). Note that in the following the assumption that $p_i^2 = 0$ is already made when presenting the amplitude. This expression shows clearly the $\sim s^2$ growth of the tree-level amplitude as $s \gg M_H^2$ if $a \neq 1$ signaling the breakdown of unitarity already at tree level when one moves away from the SM.

IV. ONE-LOOP LEVEL CALCULATION OF $w^+ w^- \rightarrow zz$

In the following, the classification of diagrams roughly follows the conventions given in Ref. [12], but of course the calculation is completely different as the nonlinear realization is used in the present paper and additional topologies of the diagrams do appear. The single diagram includes contributions from internal h , w^\pm , and z loops. We labeled by (a) the subdiagrams for the h loops and by (b) the combined ones for w^\pm and z loops.

Here, we will present the radiative corrections to the process grouped in several classes. There are the Higgs self-energy corrections to the diagram in Fig. 2 and the vertex corrections in Fig. 3. Then we have some irreducible diagrams that following [12] we classify as bubbles

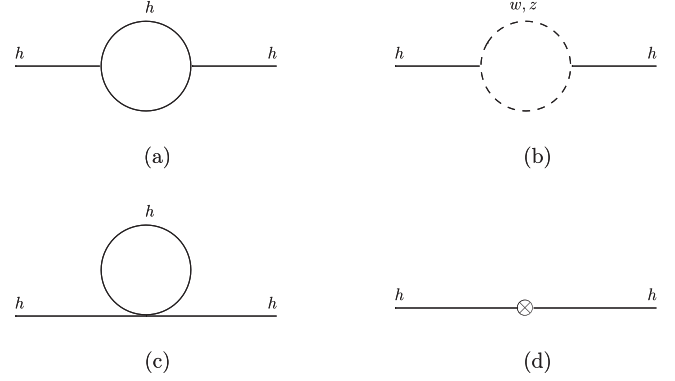


FIG. 2. Radiative corrections to the Higgs two-point function, $\mathcal{M}_{2\text{-pt}}$. (a) Contribution to $\mathcal{M}_{2\text{-pt}}^a$. (b) Contribution to $\mathcal{M}_{2\text{-pt}}^b$. (c) Contribution to $\mathcal{M}_{2\text{-pt}}^c$. (d) Contribution to $\mathcal{M}_{2\text{-pt}}^d$.

(in Fig. 4), triangles (in Fig. 5) and boxes (in Fig. 6). In addition we have two new type of diagrams that appear only in the nonlinear realization and thus have no counterpart in Ref. [12]. We have called them five-field (in Fig. 7) and six-field (in Fig. 8) diagrams, respectively.

A. Higgs self-energy corrections

The two-point diagrams given in [12] correspond to $-i\Pi(s)$ and are plotted in Fig. 2. Their contribution to the tree-level diagram $w^+ w^- \rightarrow h \rightarrow zz$ can be parametrized as

$$i\mathcal{M}_{2\text{-pt}} = \left(\frac{a}{v}\right)^2 \frac{(s)^2}{(s - M_H^2)^2} [-i\Pi(s)], \quad (10)$$

and for $d_3 = d_4 = 1$ we have

$$\begin{aligned} i\mathcal{M}_{2\text{-pt}} &= i\left(\frac{1}{4\pi v^2}\right)^2 \left(\frac{3a^2 M_H^4}{2}\right) \frac{s^2}{(s - M_H^2)^2} \\ &\times \left(\frac{A_0(M_H^2)}{M_H^2} + 3B_0(s, M_H^2, M_H^2)\right) \\ &+ a^2 \frac{s^2}{M_H^4} B_0(s, 0, 0) - i\delta M_H^2 \left(\frac{a}{v}\right)^2 \frac{s^2}{(s - M_H^2)^2}. \end{aligned} \quad (11)$$

The scalar functions A_0 and B_0 are described in the Appendix and both are ultraviolet divergent. Note that the calculation includes the counterterm for δM_H^2 (last line).

B. $hw^+ w^-$ and hzz vertex corrections

The three-point diagrams given in [12] correspond to the hww/hzz vertex correction $i\Gamma_3$, which is also related to the one-loop corrections to the Higgs decay width to

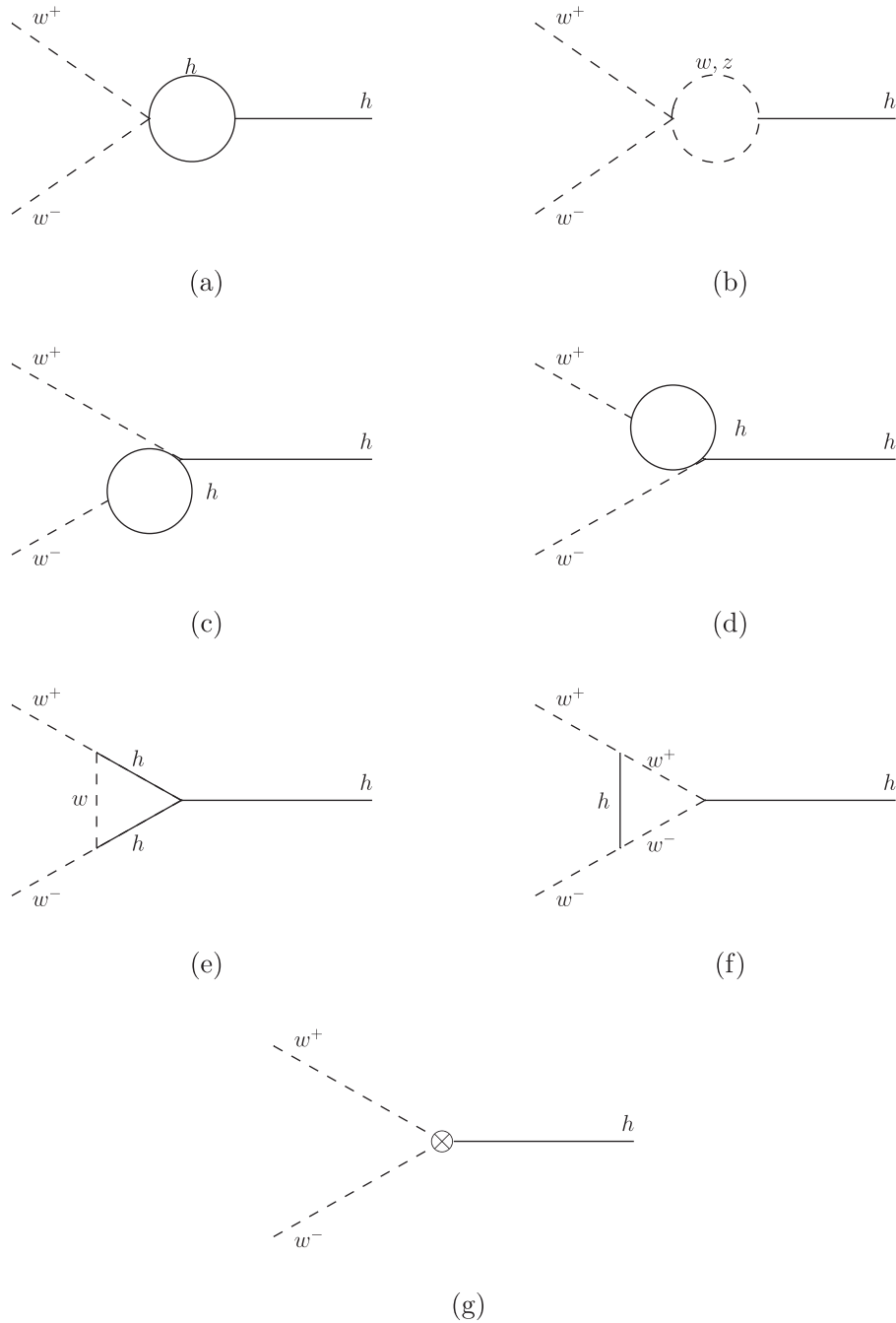


FIG. 3. Three-point vertex correction for the hw^+w^- , $\mathcal{M}_{3\text{-pt}}^a$ vertex. A slightly different set of diagrams for the vertex hzz but the result is actually the same. (a) Contribution to $\mathcal{M}_{3\text{-pt}}^a$. (b) Contribution to $\mathcal{M}_{3\text{-pt}}^b$. (c) Contribution to $\mathcal{M}_{3\text{-pt}}^c$. (d) Contribution to $\mathcal{M}_{3\text{-pt}}^d$. (e) Contribution to $\mathcal{M}_{3\text{-pt}}^e$. (f) Contribution to $\mathcal{M}_{3\text{-pt}}^f$. (g) Contribution to $\mathcal{M}_{3\text{-pt}}^g$.

ww/zz . The total correction is the same for both the hww and hzz vertices, although the actual set of diagrams is slightly different for each in the nonlinear representation, as there is a 4- w coupling but no 4- z coupling. We draw diagrams in Fig. 3 for the case of the hw^+w^- vertex. Replacing appropriately w 's by z 's lines in Fig. 3, we get the diagrams for the hzz vertex. In this case, however, we only have z internal loops in

Fig. 3(b). The rest of the diagrams are the same; however, the total correction can be given as twice the correction to any one vertex to give

$$i\mathcal{M}_{3\text{-pt}} = \left(\frac{2a}{v}\right) \frac{s}{(s - M_H^2)} [i\Gamma_3]. \quad (12)$$

We then have (for $d_3 = d_4 = 1$) the total contribution

$$\begin{aligned}
i\mathcal{M}_{3\text{-pt}} = & -i\left(\frac{1}{4\pi v^2}\right)^2 (aM_H^4)\left(\frac{s}{s-M_H^2}\right) \times \left(-a(a^2-b)\left(\frac{s}{M_H^2}\right) + 2a\left(\frac{bs-3aM_H^2}{M_H^2}\right)\frac{A_0(M_H^2)}{M_H^2}\right. \\
& + 3\left(\frac{(a^2-b)s+2a^2M_H^2}{M_H^2}\right)B_0(s, M_H^2, M_H^2) + a\left(\frac{s}{M_H^2}\right)\left(\frac{(2+a^2)s-2a^2M_H^2}{M_H^2}\right)B_0(s, 0, 0) + 2(a^3s)C_0(0, 0, s, 0, M_H^2, 0) \\
& \left. - 6(a^2M_H^2)C_0(0, 0, s, M_H^2, 0, M_H^2)\right) - i(\delta a)\left(\frac{2as}{v^2}\right)\frac{s}{(s-M_H^2)} + i\left(\frac{\delta v^2}{v^2}\right)\left(\frac{a}{v}\right)^2\frac{s^2}{(s-M_H^2)}. \quad (13)
\end{aligned}$$

Note the inclusion of the counterterms for the parameter a (describing departures from the SM hww and hzz couplings in the nonlinear realization) and for the scale v^2 . The (finite) scalar function C_0 is described in the Appendix.

C. Bubble diagrams

The bubble diagrams are given in Fig. 4 and their contributions for $d_3 = d_4 = 1$ sum up to

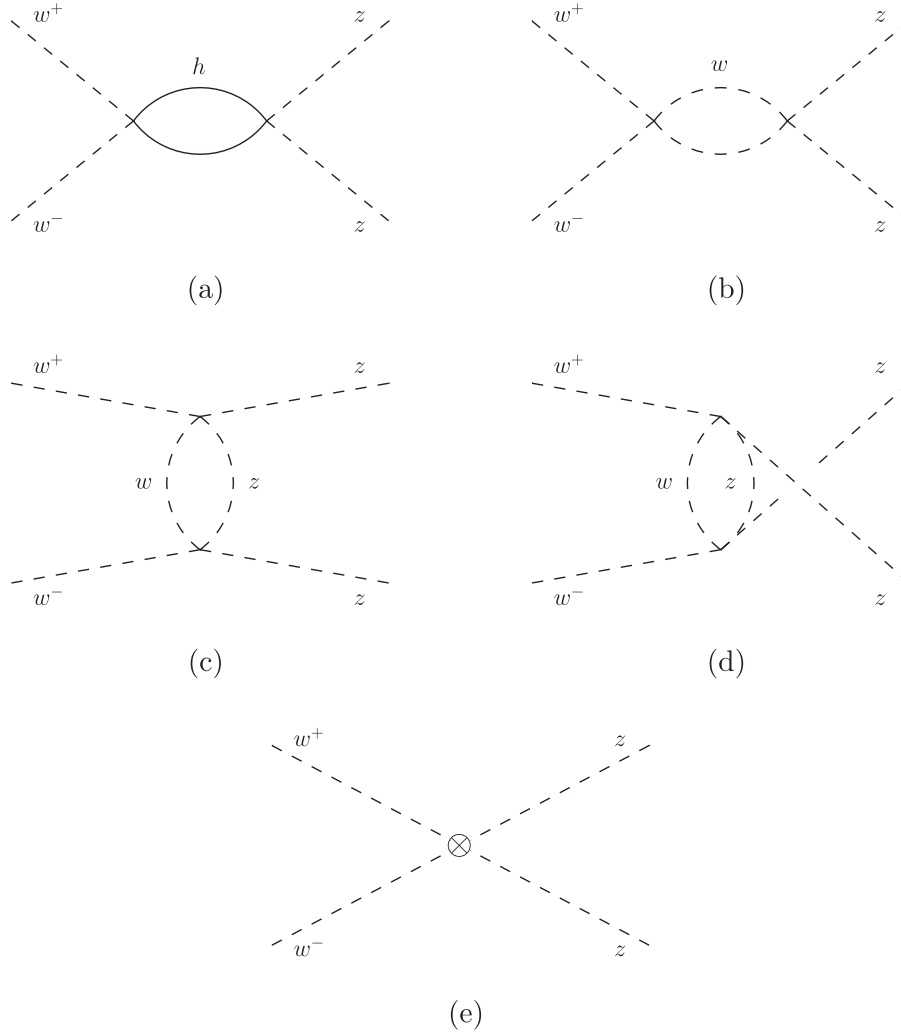


FIG. 4. Bubble diagrams, $i\mathcal{M}_{\text{bubbles}}$. Note that we have included the four-point counterterms δa_4 and δa_5 here, but this is simply a choice. (a) Contribution to $i\mathcal{M}_{\text{bubbles}}^a$. (b) Contribution to $i\mathcal{M}_{\text{bubbles}}^b$. (c) Contribution to $i\mathcal{M}_{\text{bubbles}}^c$. (d) Contribution to $i\mathcal{M}_{\text{bubbles}}^d$. (e) Contribution to $i\mathcal{M}_{\text{bubbles}}^e$.

$$\begin{aligned}
i\mathcal{M}_{\text{bubbles}} = & i\left(\frac{1}{4\pi v^2}\right)^2 \left(\frac{M_H^4}{2}\right) \times \left(\left(\frac{-2s^2 + t^2 + u^2}{9M_H^4}\right) + \left(\frac{s^2}{M_H^4}\right)(b^2 B_0(s, M_H^2, M_H^2) + B_0(s, 0, 0)) + \left(\frac{t(t-u)}{3M_H^4}\right) B_0(t, 0, 0) \right. \\
& \left. + \left(\frac{u(u-t)}{3M_H^4}\right) B_0(u, 0, 0) \right) - i\left(\frac{s}{v^2}\right)\left(\frac{\delta v^2}{v^2}\right) + i\left(\frac{4}{v^4}\right)((\delta a_4)(t^2 + u^2) + 2(\delta a_5)(s^2)). \quad (14)
\end{aligned}$$

Note the inclusion here of the counterterms for the $O(p^4)$ coefficients a_4 and a_5 .

D. Triangle diagrams

The triangle diagrams are given in Fig. 5 and their contributions give (for $d_3 = d_4 = 1$) the total result

$$\begin{aligned}
i\mathcal{M}_{\text{triangles}} = & i\left(\frac{1}{4\pi v^2}\right)^2 (a^2 M_H^4) \times \left(\frac{2s^2 - t^2 - u^2 - 18M_H^2 s}{9M_H^4} - 2\left(2\frac{s^2}{tu} - (1+b)\frac{s}{M_H^2} - 2\right) \frac{A_0(M_H^2)}{M_H^2} \right. \\
& - \frac{bs}{M_H^2} \left(\frac{s + 2M_H^2}{M_H^2}\right) B_0(s, M_H^2, M_H^2) + \frac{s}{M_H^2} \left(\frac{s - 2M_H^2}{M_H^2}\right) B_0(s, 0, 0) \\
& + \left(\frac{1}{3}\left(-\frac{t(t-u)}{M_H^4} + 3\frac{t}{M_H^2} - 6\frac{(2s+t)}{t}\right) B_0(t, 0, 0) + (t \leftrightarrow u) \right) + 2s(bC_0(0, 0, s, M_H^2, 0, M_H^2) \\
& \left. - C_0(0, 0, s, 0, M_H^2, 0)) + \left(2\left(-\frac{s}{M_H^2} - \frac{(2s+t)}{t}\right) M_H^2 C_0(0, 0, t, 0, M_H^2, 0) + (t \leftrightarrow u) \right) \right). \quad (15)
\end{aligned}$$

E. Box diagrams

The box diagrams are depicted in Fig. 6 and their contributions differ only in the exchange of $t \leftrightarrow u$,

$$\begin{aligned}
i\mathcal{M}_{\text{boxes}} = & i\left(\frac{1}{4\pi v^2}\right)^2 (a^4 M_H^4) \times \left(\frac{1}{18} \left(-\left(\frac{s}{M_H^2}\right)^2 + \left(\frac{t}{M_H^2}\right)^2 + 9\left(\frac{s}{M_H^2}\right) \right) + \left(-\frac{3}{2} \frac{s}{M_H^2} + 4\frac{t}{u} \right) \frac{A_0(M_H^2)}{M_H^2} \right. \\
& + \frac{1}{4} \left(\frac{s}{M_H^2} + 2\right)^2 B_0(s, M_H^2, M_H^2) + \left(\frac{1}{6} \frac{t(t-u)}{M_H^4} - \frac{t}{M_H^2} - 4\frac{t}{u} - 1\right) B_0(t, 0, 0) \\
& - \left(\frac{s}{M_H^2} + 2\right) M_H^2 C_0(0, 0, s, M_H^2, 0, M_H^2) + 2\left(\frac{s}{M_H^2} - \frac{u}{t}\right) M_H^2 C_0(0, 0, t, 0, M_H^2, 0) \\
& \left. + M_H^4 D_0(0, 0, 0, 0, s, t, M_H^2, 0, M_H^2, 0) \right) + (t \leftrightarrow u). \quad (16)
\end{aligned}$$

The scalar function D_0 is also described in the Appendix.

F. Five-field diagrams

The five-field diagrams do not have a linear calculation counterpart; they are a new topology present in the non-linear description. They are shown in Fig. 7 and they are found by starting from the $wwzz$ four-point vertex and adding a Higgs leg to the central vertex and then connecting it to each of the four external legs. Their inclusion is necessary to make the calculation complete to $\mathcal{O}((M_H/v)^4)$. Summed together they give

$$i\mathcal{M}_{5F} = i\left(\frac{1}{4\pi v^2}\right)^2 (a^2 M_H^4) \left(\frac{s}{M_H^2}\right) \left(1 + 2\frac{A_0(M_H^2)}{M_H^2}\right). \quad (17)$$

G. Six-field diagram

Finally, there is a single diagram here in which two Higgs legs connect to the central $wwzz$ four-point vertex

and then connect to each other to form a single closed loop. As with the five-field case, it is again necessary to ensure the calculation is complete to $\mathcal{O}((M_H/v)^4)$ and similarly has no linear-calculation counterpart. This is given in Fig. 8. It gives

$$i\mathcal{M}_{6F} = i\left(\frac{1}{4\pi v^2}\right)^2 (bM_H^4) \left(\frac{s}{M_H^2}\right) \left(\frac{-A_0(M_H^2)}{M_H^2}\right). \quad (18)$$

V. WAVE-FUNCTION RENORMALIZATION AND TADPOLES

A. Tadpoles

The one-loop tadpole diagram and counterterm are given in Fig. 9. For $M_w = 0$, and when assuming the relationship $\lambda = \frac{M^2}{2v^2}$ for the renormalized quantities, there is a single contributing diagram to the Higgs tadpole at one loop: a Higgs loop deriving from a three-Higgs coupling.

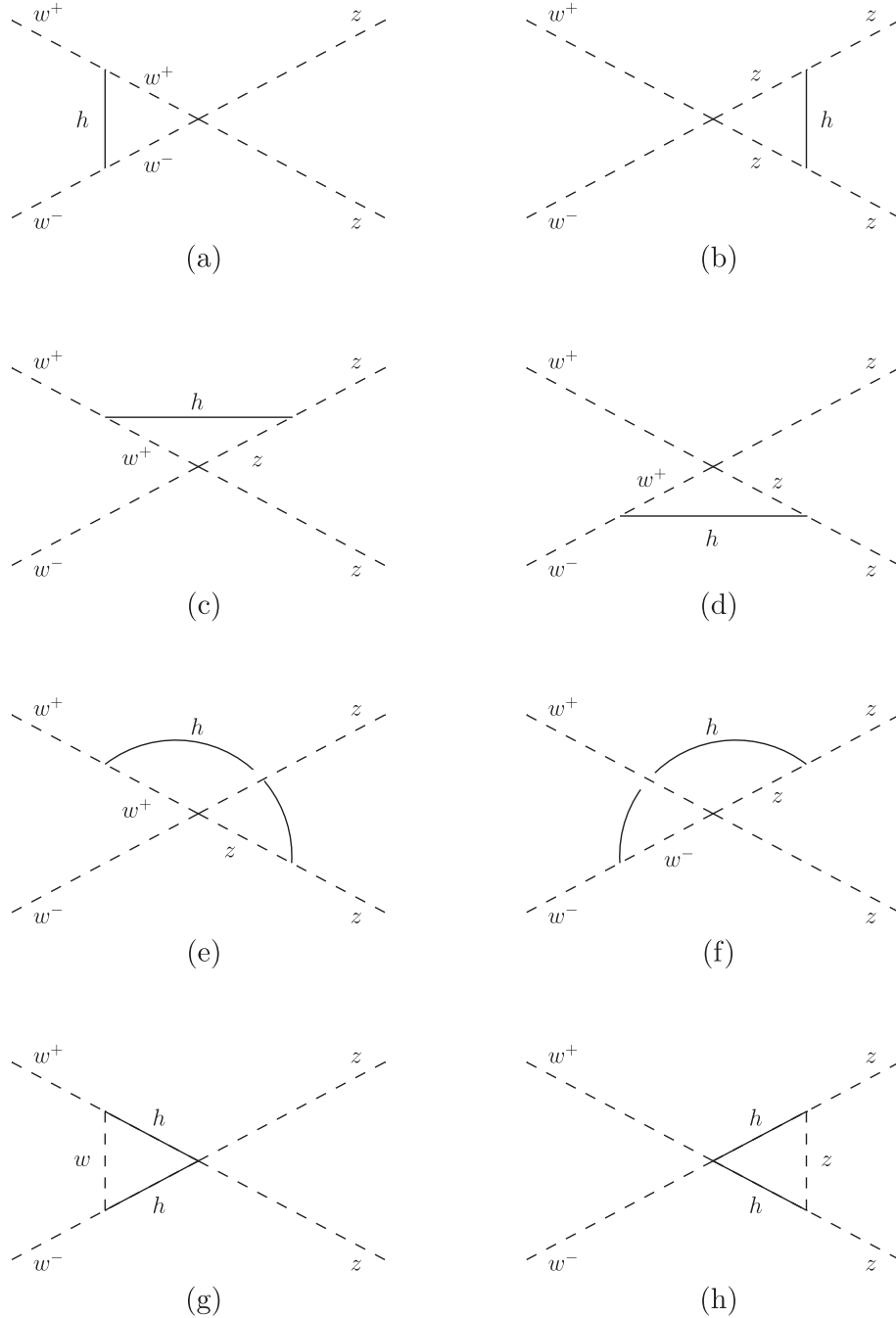


FIG. 5. Triangle diagrams contributing to the irreducible part of the $w^+ w^- \rightarrow z z$ amplitude, $i\mathcal{M}_{\text{triangles}}$. (a) Contribution to $i\mathcal{M}_{\text{triangles}}^a$. (b) Contribution to $i\mathcal{M}_{\text{triangles}}^b$. (c) Contribution to $i\mathcal{M}_{\text{triangles}}^c$. (d) Contribution to $i\mathcal{M}_{\text{triangles}}^d$. (e) Contribution to $i\mathcal{M}_{\text{triangles}}^e$. (f) Contribution to $i\mathcal{M}_{\text{triangles}}^f$. (g) Contribution to $i\mathcal{M}_{\text{triangles}}^g$. (h) Contribution to $i\mathcal{M}_{\text{triangles}}^h$.

This gives a value of the tadpole (with external leg removed) of

$$\begin{aligned}
 iT &= \left(\frac{3d_3 M_H^2}{2v} \right) \int \frac{d^{4-\epsilon} k}{(2\pi)^{4-\epsilon}} \frac{1}{(k^2 - M_H^2)} \\
 &= i \left(\frac{1}{4\pi v^2} \right)^2 \left(\frac{3M_H^2 v^3}{2} \right) A_0(M_H^2). \quad (19)
 \end{aligned}$$

From the counterterm Lagrangian Eq. (5) the contribution from the tadpole counterterm is

$$i\delta T = -iv(\delta M_H^2 - 2v^2 \delta \lambda - 2\lambda \delta v^2). \quad (20)$$

Therefore, to meet our renormalization condition for vanishing tadpoles at one loop, we must have

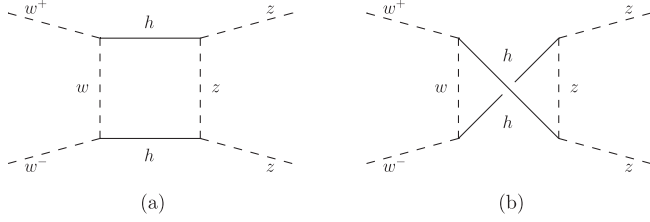


FIG. 6. The box diagrams contributing to the irreducible part of the amplitude, $i\mathcal{M}_{\text{boxes}}$. (a) Contribution to $i\mathcal{M}_{\text{boxes}}^a$. (b) Contribution to $i\mathcal{M}_{\text{boxes}}^b$.

$$\frac{\delta M_H^2}{M_H^2} - \frac{\delta \lambda}{\lambda} - \frac{\delta v^2}{v^2} = -\frac{M_H^2}{(4\pi v)^2} \left(\frac{3}{2}\right) \frac{A_0(M_H^2)}{M_H^2}. \quad (21)$$

B. Goldstone boson wave-function renormalization

When all Higgs tadpoles are appropriately canceled, there are only mixed Higgs/Goldstone boson loops, a Higgs loop, and w/z loops (which are zero when the w/z are massless). Any divergences which appear due to the wave-function renormalization of the external fields must be canceled by something in the remainder of this amplitude. We shall see later that this is easily achieved with the renormalization of v^2 , which is also a global factor multiplying the tree-level contribution. In fact from the mere requirement of finiteness of the amplitude after including the one-loop diagrams, we can derive only a condition on the combination $2\delta Z_w - \delta v^2$. Therefore the renormalization condition on the wave function has to be imposed separately and this consists in requesting the unit residue condition on the external legs.

The two-point function for the Goldstone bosons in Fig. 10 gives the following:

$$\begin{aligned} -i\Pi_w(q^2) &\equiv -i\Pi_w^{(1+2)}(q^2) \\ &= i\left(\frac{1}{4\pi v^2}\right)^2 (v^2)((a^2(3q^2 - M_H^2) - bq^2)A_0(M_H^2) \\ &\quad + a^2(q^2 - M_H^2)^2 B_0(q^2, 0, M_H^2)), \end{aligned} \quad (22)$$

which verifies $\Pi_w(0) = 0$ for all a and b , and therefore the Goldstone bosons stay massless, as they should.⁵

The wave-function renormalization factor is then

$$\begin{aligned} Z_w &= 1 + \frac{d\Pi_w}{dq^2} \Big|_{q^2=0} \\ &= 1 - \left(\frac{1}{4\pi v}\right)^2 \left((a^2 - b)A_0(M_H^2) + a^2 \frac{M_H^2}{2}\right). \end{aligned} \quad (23)$$

In the SM case, this is finite and matches the value given by Ref. [13]

$$Z_w^{\text{SM}} = \left(1 - \left(\frac{1}{4\pi v}\right)^2 \left(\frac{M_H^2}{2}\right)\right) = \left(1 - \frac{\lambda^2}{16\pi^2}\right), \quad (24)$$

⁵To see this, it is important to note that $B_0(0, 0, M_H^2) = A_0(M_H^2)/M_H^2$.

but in general it is divergent. This divergence is canceled against contributions from δv^2 when the corresponding contribution to the one-loop amplitude is placed in the complete calculation. The one-loop contribution to the amplitude $w^+ w^- \rightarrow z z$ from wave-function renormalization is

$$\begin{aligned} i\mathcal{M}_{\text{WFR}} &= i\left(\frac{1}{4\pi v^2}\right)^2 (M_H^2 s) \left(\frac{(a^2 - 1)s + M_H^2}{s - M_H^2}\right) \\ &\quad \times \left(a^2 + 2(a^2 - b) \frac{A_0(M_H^2)}{M_H^2}\right). \end{aligned} \quad (25)$$

C. Higgs boson wave-function renormalization

The contributions to the Higgs two-point function can be derived from Sec. IV A, while the counterterm contribution is simply

$$-i\Pi_H^{(\text{ctr})}(q^2) = -i\delta M_H^2. \quad (26)$$

This gives

$$\begin{aligned} -i\Pi_H(q^2) &= i\left(\frac{1}{4\pi v}\right)^2 \left(\frac{3M_H^4}{2}\right) \left(\frac{d_4}{M_H^2} A_0(M_H^2)\right. \\ &\quad + 3d_3^2 B_0(q^2, M_H^2, M_H^2) \\ &\quad \left.+ a^2 \frac{s^2}{M_H^4} B_0(q^2, 0, 0)\right) - i\delta M_H^2. \end{aligned} \quad (27)$$

The on-shell condition for the Higgs mass requires

$$\text{Re}\Pi_H(M_H^2) = 0. \quad (28)$$

Independent of this condition and the counterterm, we have the wave-function renormalization factor of (now setting $d_3 = d_4 = 1$)

$$\begin{aligned} Z_H &= 1 + \frac{d\Pi_H}{dq^2} \Big|_{q^2=M_H^2} \\ &= 1 - \left(\frac{1}{4\pi v}\right)^2 \left(\frac{3M_H^4}{2}\right) \left(3B_0'(M_H^2, M_H^2, M_H^2)\right. \\ &\quad \left.+ a^2 \left(B_0'(M_H^2, 0, 0) + \frac{2}{M_H^2} B_0(M_H^2, 0, 0)\right)\right) \\ &= 1 + \left(\frac{M_H}{4\pi v}\right)^2 \left(\left(\frac{9}{2}\right) \left(1 - \frac{2\sqrt{3}\pi}{9}\right)\right. \\ &\quad \left.+ a^2 \left(\frac{3}{2} - B_0(M_H^2, 0, 0)\right)\right). \end{aligned} \quad (29)$$

This is divergent in the SM case and only becomes finite for $a = 0$. When the one-loop correction to $i\Gamma(h \rightarrow w^+ w^-)$ is performed and all external wave-function renormalizations are included (i.e. both Z_H and Z_w), all divergences cancel for arbitrary a and b when using the appropriate values for the counterterms given in Sec. VI. This is a good check on this value of Z_H . It should also be noted that the SM value for Z_H does not match that

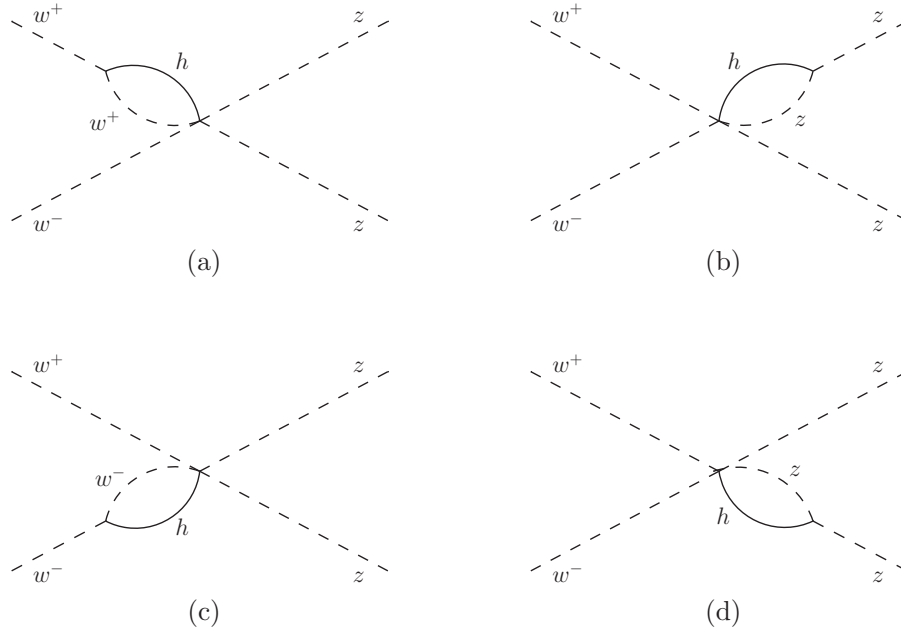


FIG. 7. Five-field diagrams, $i\mathcal{M}_{5F}$. Note that they do not have a counterpart in the linear realization of the SM. (a) Contribution to $i\mathcal{M}_{5F}^a$. (b) Contribution to $i\mathcal{M}_{5F}^b$. (c) Contribution to $i\mathcal{M}_{5F}^c$. (d) Contribution to $i\mathcal{M}_{5F}^d$.

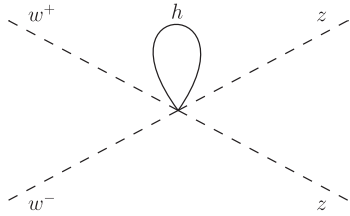


FIG. 8. Six-field diagram, $i\mathcal{M}_{6F}$.

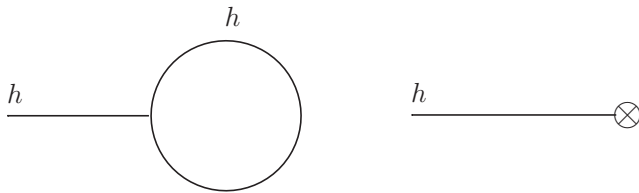


FIG. 9. Tadpole diagram and counterterm for the Higgs field.

given in Ref. [13]; this is a result of the nonlinear nature of the calculation.

The complete, renormalized decay width for the Higgs boson into Goldstone bosons is

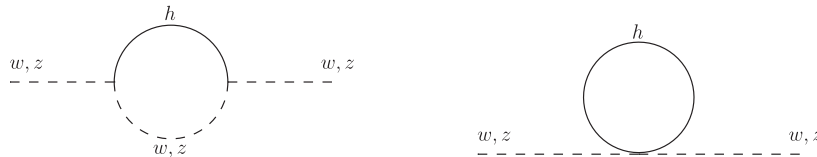


FIG. 10. Self-energy for w/z fields (contribution to $i\mathcal{M}_{\text{WFR}}$).

$$\begin{aligned} \Gamma(h \rightarrow ww) = & \left(\frac{3\lambda M_H a}{16\pi} \right) \left(a + \left(\frac{\lambda}{\pi^2} \right) \left\{ \left(\frac{1}{16} \right) (a(17 + 10b) \right. \right. \\ & - 3a(7a - 8) - 2\overline{\delta v^2}) - 12b \right\} \\ & \left. - \left(\frac{\pi}{8} \right) \sqrt{3}(1 + 3a - b) + \left(\frac{\pi^2}{48} \right) (a^2)(4 + a) \right\} \end{aligned} \quad (30)$$

for arbitrary a and b , where $\overline{\delta v^2}$ is a finite renormalization, not fixed by our conditions. For $a = b = 1$ and $\overline{\delta v^2} = -\frac{1}{2}$ (the value used in Refs. [12,13]), this reproduces the known SM result

$$\Gamma(h \rightarrow ww) = \left(\frac{3\lambda M_H}{16\pi} \right) \left(1 + \left(\frac{\lambda}{\pi^2} \right) \left\{ \frac{19}{16} - \frac{3\sqrt{3}\pi}{8} + \frac{5\pi^2}{48} \right\} \right). \quad (31)$$

VI. DIVERGENCES AND DETERMINATION OF THE COUNTERTERMS

Here we give the pieces of each individual diagram proportional to $\Delta_\epsilon = \left(\frac{2}{\epsilon} \right) - \gamma_E + \log 4\pi + \log \frac{\mu^2}{M_H^2}$. We give the results in the case $d_3 = d_4 = 1$ but it is quite straightforward to restore these factors for each individual

diagram if so desired. These factors appear only in the radiative corrections to two- and three-point functions,

$$\begin{aligned}\mathcal{M}_{2\text{-pt}}^{(a)} &\sim \left(\frac{1}{4\pi v^2}\right)^2 \Delta_\epsilon \left(\frac{9a^2 M_H^4 s^2}{2(s - M_H^2)^2}\right), \\ \mathcal{M}_{2\text{-pt}}^{(b)} &\sim \left(\frac{1}{4\pi v^2}\right)^2 \Delta_\epsilon \left(\frac{3a^4 s^4}{2(s - M_H^2)^2}\right), \\ \mathcal{M}_{2\text{-pt}}^{(c)} &\sim \left(\frac{1}{4\pi v^2}\right)^2 \Delta_\epsilon \left(\frac{3a^2 M_H^4 s^2}{2(s - M_H^2)^2}\right),\end{aligned}\quad (32)$$

$$\begin{aligned}\mathcal{M}_{3\text{-pt}}^{(a)} &\sim \left(\frac{1}{4\pi v^2}\right)^2 \Delta_\epsilon \left(\frac{3ab M_H^2 s^2}{(s - M_H^2)}\right), \\ \mathcal{M}_{3\text{-pt}}^{(b)} &\sim \left(\frac{1}{4\pi v^2}\right)^2 \Delta_\epsilon \left(\frac{-2a^2 s^3}{(s - M_H^2)}\right), \\ \mathcal{M}_{3\text{-pt}}^{(c)} &\sim \left(\frac{1}{4\pi v^2}\right)^2 \Delta_\epsilon \left(\frac{-2a^2 b M_H^2 s^2}{(s - M_H^2)}\right), \\ \mathcal{M}_{3\text{-pt}}^{(d)} &\sim \left(\frac{1}{4\pi v^2}\right)^2 \Delta_\epsilon \left(\frac{-3a^3 M_H^2 s^2}{(s - M_H^2)}\right), \\ \mathcal{M}_{3\text{-pt}}^{(e)} &\sim \left(\frac{1}{4\pi v^2}\right)^2 \Delta_\epsilon \left(\frac{-a^4 s^2 (s - 2M_H^2)}{(s - M_H^2)}\right),\end{aligned}\quad (33)$$

$$\begin{aligned}\mathcal{M}_{\text{bubble}}^{(a)} &\sim \left(\frac{1}{4\pi v^2}\right)^2 \Delta_\epsilon \left(\frac{b^2 s^2}{2}\right), \\ \mathcal{M}_{\text{bubble}}^{(b)} &\sim \left(\frac{1}{4\pi v^2}\right)^2 \Delta_\epsilon \left(\frac{s^2}{2}\right), \\ \mathcal{M}_{\text{bubble}}^{(c)} &\sim \left(\frac{1}{4\pi v^2}\right)^2 \Delta_\epsilon \left(\frac{t(t - u)}{6}\right), \\ \mathcal{M}_{\text{bubble}}^{(d)} &\sim \left(\frac{1}{4\pi v^2}\right)^2 \Delta_\epsilon \left(\frac{u(u - t)}{6}\right),\end{aligned}\quad (34)$$

$$\begin{aligned}\mathcal{M}_{\text{triangle}}^{(a)+(b)} &\sim \left(\frac{1}{4\pi v^2}\right)^2 \Delta_\epsilon \left(\frac{a^2 s (3s - 2M_H^2)}{3}\right), \\ \mathcal{M}_{\text{triangle}}^{(c)+(d)} &\sim \left(\frac{1}{4\pi v^2}\right)^2 \Delta_\epsilon \left(\frac{-a^2 t ((t - u) - M_H^2)}{3}\right), \\ \mathcal{M}_{\text{triangle}}^{(e)+(f)} &\sim \left(\frac{1}{4\pi v^2}\right)^2 \Delta_\epsilon \left(\frac{-a^2 u ((u - t) - M_H^2)}{3}\right), \\ \mathcal{M}_{\text{triangle}}^{(g)+(h)} &\sim \left(\frac{1}{4\pi v^2}\right)^2 \Delta_\epsilon (-a^2 b s^2),\end{aligned}\quad (35)$$

$$\mathcal{M}_{\text{box}}^{(a)+(b)} \sim \left(\frac{1}{4\pi v^2}\right)^2 \Delta_\epsilon \left(\frac{a^4 (s^2 + t^2 + u^2)}{3}\right), \quad (36)$$

$$\mathcal{M}_{5F}^{(a)+(b)+(c)+(d)} \sim \left(\frac{1}{4\pi v^2}\right)^2 \Delta_\epsilon (2a^2 M_H^2 s), \quad (37)$$

$$\mathcal{M}_{6F} \sim \left(\frac{1}{4\pi v^2}\right)^2 \Delta_\epsilon (-b M_H^2 s), \quad (38)$$

$$\mathcal{M}_{\text{WFR}} \sim \left(\frac{1}{4\pi v^2}\right)^2 \Delta_\epsilon (2M_H^2 s) (a^2 - b) \left(\frac{(a^2 - 1)s + M_H^2}{(s - M_H^2)}\right). \quad (39)$$

Note that we have included the w , z Goldstone boson wave-function renormalization as a contribution to the one-loop amplitude to be canceled by the counterterms in $\delta\mathcal{L}$.

If we ignore the tadpole counterterms, we can collect together all the individual counterterms to give the following:

$$\begin{aligned}\mathcal{M}^{\text{ctr}} &= \left(\frac{1}{v^2}\right) \left(\frac{s}{(s - M_H^2)}\right) \left(\frac{\delta v^2}{v^2} ((a^2 - 1)s^2\right. \\ &\quad + (2 - a^2)(sM_H^2) - M_H^4) - \delta a((2a)(s)(s - M_H^2)) \\ &\quad - \frac{\delta M_H^2}{M_H^2} ((a^2)(sM_H^2)) \left. + \left(\frac{1}{v^4}\right) (4\delta a_4(t^2 + u^2)\right. \\ &\quad \left. + 8\delta a_5(s^2))\right).\end{aligned}\quad (40)$$

The values of the counterterms needed to cancel the one-loop divergences—and satisfy our renormalization conditions—can be solved for arbitrary a and b to give

$$\begin{aligned}\frac{\delta v^2}{v^2} &= \frac{M_H^2}{(4\pi v)^2} (\Delta_\epsilon (-a^2 + b) + \overline{\delta v^2}), \\ \frac{\delta M_H^2}{M_H^2} &= \frac{M_H^2}{(4\pi v)^2} \left(\frac{3}{2}\right) (\Delta_\epsilon (4 + a^2) + 7 + 2a^2 - \sqrt{3}\pi), \\ \frac{\delta\lambda}{\lambda} &= \frac{M_H^2}{(4\pi v)^2} \left(\frac{1}{2}\right) (\Delta_\epsilon (9 + 5a^2 - 2b) + 18 \\ &\quad + 6a^2 - 3\sqrt{3}\pi - 2\overline{\delta v^2}), \\ \delta a &= \frac{M_H^2}{(4\pi v)^2} \left(\frac{1}{2}\right) (\Delta_\epsilon (a - 1)(a(5a + 2) - 3b)), \\ \delta a_4 &= \frac{1}{(4\pi)^2} \left(\frac{-1}{12}\right) (\Delta_\epsilon (a^2 - 1)^2), \\ \delta a_5 &= \frac{1}{(4\pi)^2} \left(\frac{-1}{48}\right) (\Delta_\epsilon (2 + 5a^4 - 4a^2 - 6a^2 b + 3b^2)),\end{aligned}\quad (41)$$

where $\overline{\delta v^2}$ is a finite piece, not determined by the renormalization conditions *a priori*. Note that the counterterm for b cannot be determined from this process. As previously indicated it is quite easy to restore the dependence on d_3 and d_4 in the divergent part of all diagrams but we will not present the results here.

A. Cross-checks

In the SM case ($a = b = 1$), renormalization conditions read as

$$\begin{aligned}\frac{\delta v^2}{v^2} &= \frac{M_H^2}{(4\pi v)^2} (\overline{\delta v^2}), \\ \frac{\delta M_H^2}{M_H^2} &= \frac{M_H^2}{(4\pi v)^2} \left(\frac{3}{2}\right) (\Delta_\epsilon (5) + 9 - \sqrt{3}\pi), \\ \frac{\delta\lambda}{\lambda} &= \frac{M_H^2}{(4\pi v)^2} \left(\Delta_\epsilon (6) + 12 - \frac{3}{2}\sqrt{3}\pi - \overline{\delta v^2}\right), \\ \delta a &= 0, \quad \delta a_4 = 0, \quad \delta a_5 = 0.\end{aligned}\quad (42)$$

The last three terms should be absent in the SM, so this is a good check. In the EChL case ($a = b = 0$) we have

$$\begin{aligned}\frac{\delta v^2}{v^2} &= \frac{M_H^2}{(4\pi v)^2} (\overline{\delta v^2}), \\ \frac{\delta M_H^2}{M_H^2} &= \frac{M_H^2}{(4\pi v)^2} \left(\frac{3}{2}\right) (\Delta_\epsilon(4) + 7 - \sqrt{3}\pi), \\ \frac{\delta\lambda}{\lambda} &= \frac{M_H^2}{(4\pi v)^2} \left(\Delta_\epsilon\left(\frac{9}{2}\right) + 9 - \frac{3}{2}\sqrt{3}\pi - \overline{\delta v^2}\right), \quad \delta a = 0 \\ \delta a_4 &= \frac{1}{(4\pi)^2} \Delta_\epsilon\left(\frac{-1}{12}\right), \quad \delta a_5 = \frac{1}{(4\pi)^2} \Delta_\epsilon\left(\frac{-1}{24}\right),\end{aligned}\quad (43)$$

in agreement with already known results [4].

It is interesting to note here that while $\delta M_H^2 \neq 0$, its contribution to the counterterm amplitude is actually

proportional to a^2 and therefore vanishes when $a \rightarrow 0$ [see Eq. (40)]. Also, the $\delta\lambda$ term is only necessary here to remove the tadpole divergence (which is absent from the full amplitude for $a = b = 0$) so once again plays no part. Finally, the δv^2 term is finite. Therefore only δa_4 and δa_5 are needed to remove the one-loop divergences from the Goldstone boson scattering amplitudes, which is what one would expect in the EChL approach.

VII. FINAL RESULT AND CONCLUSIONS

Finally, the complete one-loop amplitude $i\mathcal{M}^{\text{loop}}(w^+ w^- \rightarrow zz)$ [for arbitrary a and b and rendered finite by using the counterterms in Eq. (41)] is given by the following:

$$\begin{aligned}i\mathcal{M}^{\text{loop}} &= i \left(\frac{1}{4\pi v^2}\right)^2 \left(\frac{M_H^2}{2}\right)^2 \left(\frac{6a^2(-6-2a^2+\sqrt{3}\pi)M_H^4}{(s-M_H^2)^2} - \frac{4a^2(18+2a(a-3)+5b-3\sqrt{3}\pi-\overline{\delta v^2})M_H^2}{(s-M_H^2)}\right. \\ &\quad - \frac{2}{9}(a^2-1)\left((a^2-1)\frac{t^2+4tu+u^2}{M_H^4} - 72a^2\frac{t^2+tu+u^2}{tu}\right) + 4\left(\frac{s}{M_H^2}\right)(2a^4-3a^2b+b+(a^2-1)\overline{\delta v^2}) \\ &\quad + a^2(6\sqrt{3}\pi-4(9+3a(a-2)+5b-\overline{\delta v^2})) + 2\left(\frac{(a^2-b)s^2+((a^2-b)-3a)M_H^2s-2a^2M_H^4}{M_H^2(s-M_H^2)}\right)^2 \bar{B}_0(s, M_H^2, M_H^2) \\ &\quad + 2\frac{s((a^2-1)s+M_H^2)}{M_H^4} \left(\frac{(a^2-1)s^2+(6a^2+1)M_H^2s-4a^2M_H^4}{(s-M_H^2)^2}\right) \bar{B}_0(s, 0, 0) \\ &\quad + \left(\left(\frac{4(a^2-1)^2}{3}\frac{t^2}{M_H^4} + \frac{2(a^2-1)((a^2-1)s-6a^2M_H^2)}{3M_H^2}\frac{t}{M_H^2} + 4a^2(1-(a^2-1)(1+4\frac{u}{t})\right)\right) \bar{B}_0(t, 0, 0) + (t \Leftrightarrow u) \\ &\quad - 8a^2\frac{(a^2-b)s^2+((a^2-b)-3a)M_H^2s-2a^2M_H^4}{(s-M_H^2)} C_0(0, 0, s, M_H^2, 0, M_H^2) \\ &\quad + 8a^2\frac{s}{(s-M_H^2)}((a^2-1)s+M_H^2)C_0(0, 0, s, 0, M_H^2, 0) + \left(8a^2((a^2-1)s+M_H^2\left(1-2(a^2-1)\frac{u}{t}\right))\right) C_0(0, 0, t, 0, M_H^2, 0) \\ &\quad + (t \Leftrightarrow u) + (4a^2M_H^4 D_0(0, 0, 0, 0, s, t, M_H^2, 0, M_H^2, 0) + (t \Leftrightarrow u)).\end{aligned}\quad (44)$$

Here the functions \bar{A}_0 and \bar{B}_0 are the corresponding scalar integral functions with the divergences removed (see Appendix). The amplitude as written above has been grouped by scalar loop integrals. In the SM limit ($a = b = 1$), this simplifies quite a bit

$$\begin{aligned}i\mathcal{M}_{\text{SM}}^{\text{loop}} &= i \left(\frac{1}{4\pi v^2}\right)^2 \left(\frac{M_H^2}{2}\right)^2 \left(+\frac{M_H^4}{(s-M_H^2)^2}(-48+6\sqrt{3}\pi+18\bar{B}_0(s, M_H^2, M_H^2)+6\bar{B}_0(s, 0, 0))\right. \\ &\quad + \frac{M_H^2}{(s-M_H^2)}(-76+12\sqrt{3}\pi+4\overline{\delta v^2}+12\bar{B}_0(s, M_H^2, M_H^2)+20\bar{B}_0(s, 0, 0)+(8M_H^2)(3C_0(0, 0, s, M_H^2, 0, M_H^2) \\ &\quad + C_0(0, 0, s, 0, M_H^2, 0))) + (2\bar{B}_0(s, M_H^2, M_H^2)+14\bar{B}_0(s, 0, 0)+4\bar{B}_0(t, 0, 0)+4\bar{B}_0(u, 0, 0)) \\ &\quad + (8M_H^2)(C_0(0, 0, s, M_H^2, 0, M_H^2)+C_0(0, 0, s, 0, M_H^2, 0)+C_0(0, 0, t, 0, M_H^2, 0)+C_0(0, 0, u, 0, M_H^2, 0)) \\ &\quad \left.+ (4M_H^4)(D_0(0, 0, 0, 0, s, t, M_H^2, 0, M_H^2, 0)+D_0(0, 0, 0, 0, s, u, M_H^2, 0, M_H^2, 0))-2(22-3\sqrt{3}\pi-2\overline{\delta v^2})\right).\end{aligned}\quad (45)$$

Equations (41) and (44) contain our main results. We have seen how the departures from the SM can be taken consistently into account in an effective-Lagrangian philosophy also at the one-loop level and the suitable counterterms included to render the amplitude finite. We note that if a and b are set to their SM values, the coefficients accompanying the $O(p^4)$ operators are finite and do not run, while this is not the case as soon as one departs from the SM. After cancellation of the divergent part of the loop (say in the $\overline{\text{MS}}$ scheme), a finite logarithmic part remains. For instance in the case of the effective coefficients a_4 and a_5 , and appealing to naturality arguments, their characteristic size would be

$$\begin{aligned}\delta a_4 &= \frac{1}{(4\pi)^2} \left(\frac{-1}{12} \right) (a^2 - 1)^2 \log \frac{f^2}{v^2}, \\ \delta a_5 &= \frac{1}{(4\pi)^2} \left(\frac{-1}{48} \right) (2 + 5a^4 - 4a^2 - 6a^2b + 3b^2) \log \frac{f^2}{v^2},\end{aligned}\quad (46)$$

with f being the compositeness scale.

In the present study we have restricted ourselves to the case where the triple and quartic Higgs coupling take the same values as in the SM, but relaxing this hypothesis is straightforward. The dependence of the divergent parts on d_3 and d_4 can be easily determined as they simply contribute as overall factors to vertex and self-energy corrections. None of those diagrams behave as $\sim s^2$ (or as t^2 or u^2) for large values of s , and they therefore do not contribute to δa_4 and δa_5 that are totally independent of d_3 and d_4 .

It would be interesting to extend the present study to other low-energy constants of the effective theory parametrizing the EWSBS. In particular, a_1 and a_2 correspond to operators that contribute to the triple gauge boson vertex that has been recently measured for the first time at the LHC [14]. The renormalization of d_3 and d_4 would eventually be of interest too, but their relevance for comparison with experiment is still well ahead.

We have also presented a full one-loop calculation using the equivalence theorem approximation (and taking the masses of the Goldstone bosons to vanish, i.e. in the 't Hooft-Landau gauge) of the $W_L W_L \rightarrow Z_L Z_L$ in the general case with generic couplings of the Higgs to

the electroweak gauge bosons. This calculation should be quite useful in precise comparisons of measurements of the four gauge boson coupling (not yet measured at the LHC) to theoretical predictions. Its knowledge is also very relevant in connection with unitarity analysis such as the one done in [1] and the prediction of new resonances originating from the EWSBS. As emphasized in the Introduction, the search for such resonances has to go hand in hand with accurate measurements of the four gauge boson couplings. Almost any deviation of these coefficients from their SM values would lead to unitarity violations at high energies and thus require additional resonances to restore it. In a forthcoming publication we will study in detail the issue of unitarity and extend the results of [1] to the case where the tree-level $O(p^2)$ parameters a and b depart from their SM values. Both the determination of the counterterms and the full calculation of the real part of the scattering amplitude derived in this preparatory paper are necessary ingredients for such an analysis.

In conclusion, we have successfully provided a one-loop theory of Goldstone boson scattering in the context of an extended EWSBS where the Higgs is allowed to have arbitrary couplings. The coefficients a and b describing the coupling of the Higgs to the W and Z gauge bosons are currently of great interest to SM fits, but their treatment so far has only been of tree-level studies. If a and b are not exactly equal to 1, some $O(p^4)$ operators with running coefficients are required for a consistent treatment at one loop. Their running has been determined in this work. The results smoothly connect to the SM and are, we believe, completely general.

ACKNOWLEDGMENTS

We gratefully acknowledge the financial support from Projects No. FPA2010-20807, No. 2009SGR502, and CPAN (Consolider CSD2007-00042). We thank A. Pomarol for discussions.

APPENDIX

Here we define the independent scalar integrals entering our expressions

$$\begin{aligned}A_0(m_0^2) &= \mathcal{N} \int d^d k \frac{1}{k^2 - m_0^2} = m_0^2 (\Delta_\epsilon + 1), \\ B_0(p_1^2, m_0^2, m_1^2) &= \mathcal{N} \int d^d k \frac{1}{k^2 - m_0^2} \frac{1}{(k + p_1)^2 - m_1^2}, \\ C_0(p_1^2, p_2^2, p_{12}^2, m_0^2, \dots, m_3^2) &= \mathcal{N} \int d^d k \frac{1}{k^2 - m_0^2} \frac{1}{(k + p_1)^2 - m_1^2} \frac{1}{(k + p_{12})^2 - m_2^2},\end{aligned}\quad (A1)$$

$$D_0(p_1^2, p_2^2, p_3^2, p_{13}^2, p_{12}^2, p_{23}^2, m_0^2, \dots, m_3^2) = \mathcal{N} \int d^d k \frac{1}{k^2 - m_0^2} \frac{1}{(k + p_1)^2 - m_1^2} \frac{1}{(k + p_{12})^2 - m_2^2} \frac{1}{(k + p_{13})^2 - m_3^2}, \quad (A2)$$

where $\mathcal{N} = (2\pi\mu)^{4-d}/(i\pi^2)$ and $p_{ij} = \sum_{h=i}^j p_h$. We note that of the scalar loop integrals (A_0 , B_0 , C_0 , and D_0) in our solution only A_0 and B_0 contain divergences. We will therefore define the functions \bar{A}_0 and \bar{B}_0 as the corresponding scalar integral functions with the divergences removed

$$\begin{aligned} A_0(a) &= a\Delta_\epsilon + \bar{A}_0(a), \\ B_0(a, b, c) &= \Delta_\epsilon + \bar{B}_0(a, b, c). \end{aligned} \quad (\text{A3})$$

Note that this differs slightly from the $\Delta_\epsilon = (\frac{2}{\epsilon} - \gamma_E + \log 4\pi)$ used in the literature on the scalar

loop integrals. However, this has the benefit that all factors of $\log \frac{\mu^2}{M_H^2}$ are currently in the counterterms and that $\bar{A}_0(M_H^2) = M_H^2$. For situations in which it is better to have $\log \frac{\mu^2}{M_H^2}$ explicitly in the amplitude (for instance in the limit $M_H^2 \rightarrow \infty$), this can be achieved by replacing each counterterm in Eq. (40) with $\mathcal{C} \log \frac{\mu^2}{M_H^2}$, where \mathcal{C} is the coefficient of the divergent part of the corresponding counterterm, and then adding it to the amplitude.

-
- [1] D. Espriu and B. Yencho, *Phys. Rev. D* **87**, 055017 (2013).
- [2] G. Aad *et al.* (ATLAS Collaboration), *Phys. Lett. B* **716**, 1 (2012).
- [3] S. Chatrchyan *et al.* (CMS Collaboration), *Phys. Lett. B* **716**, 30 (2012).
- [4] A. Dobado, D. Espriu, and M.J. Herrero, *Phys. Lett. B* **255**, 405 (1991); D. Espriu and M.J. Herrero, *Nucl. Phys. B* **373**, 117 (1992); M.J. Herrero and E. Ruiz-Morales, *Nucl. Phys. B* **418**, 431 (1994); **437**, 319 (1995); D. Espriu and J. Matias, *Phys. Lett. B* **341**, 332 (1995); A. Dobado, M.J. Herrero, J.R. Peláez, and E. Ruiz-Morales, *Phys. Rev. D* **62**, 055011 (2000); R. Foadi, M. Jarvinen, and F. Sannino, *Phys. Rev. D* **79**, 035010 (2009).
- [5] G.F. Giudice, C. Grojean, A. Pomarol, and R. Rattazzi, *J. High Energy Phys.* **06** (2007), 045; R. Contino, M. Ghezzi, C. Grojean, M. Muhlleitner, and M. Spira, *J. High Energy Phys.* **07** (2013), 035; R. Alonso, M.B. Gavela, L. Merlo, S. Rigolin, and J. Yepes, *Phys. Lett. B* **722**, 330 (2013).
- [6] G. Belanger, B. Dumont, U. Ellwanger, J.F. Gunion, and S. Kraml, [arXiv:1306.2941](https://arxiv.org/abs/1306.2941); T. Corbett, O.J.P. Eboli, J. Gonzalez-Fraile, and M.C. Gonzalez-Garcia, *Phys. Rev. D* **86**, 075013 (2012); [arXiv:1306.0006](https://arxiv.org/abs/1306.0006); J. Ellis and T. You, *J. High Energy Phys.* **06** (2013), 103; P.P. Giardino, K. Kannike, I. Masina, M. Raidal, and A. Strumia, [arXiv:1303.3570](https://arxiv.org/abs/1303.3570); A. Falkowski, F. Riva, and A. Urbano, [arXiv:1303.1812](https://arxiv.org/abs/1303.1812); T. Alanne, S. Di Chiara, and K. Tuominen, [arXiv:1303.3615](https://arxiv.org/abs/1303.3615).
- [7] O. Cheyette and M.K. Gaillard, *Phys. Lett. B* **197**, 205 (1987); A. Dobado, M.J. Herrero, and T.N. Truong, *Phys. Lett. B* **235**, 129 (1990); W. Dicus and W.W. Repko, *Phys. Rev. D* **42**, 3660 (1990); **44**, 3473 (1991); **47**, 4154 (1993); J.R. Peláez, *Phys. Rev. D* **55**, 4193 (1997).
- [8] J.M. Cornwall, D.N. Levin, and G. Tiktopoulos, *Phys. Rev. D* **10**, 1145 (1974); B.W. Lee, C. Quigg, and H. Thacker, *Phys. Rev. D* **16**, 1519 (1977); G.J. Gounaris, R. Kogerler, and H. Neufeld, *Phys. Rev. D* **34**, 3257 (1986); M.S. Chanowitz and M.K. Gaillard, *Nucl. Phys. B* **261**, 379 (1985); A. Dobado and J.R. Peláez, *Nucl. Phys. B* **425**, 110 (1994); *Phys. Lett. B* **329**, 469 (1994); C. Grosse-Knetter and I. Kuss, *Z. Phys. C* **66**, 95 (1995); H.J. He, Y.P. Kuang, and X. Li, *Phys. Lett. B* **329**, 278 (1994).
- [9] D. Espriu and J. Matias, *Phys. Rev. D* **52**, 6530 (1995).
- [10] T.N. Truong, *Phys. Rev. Lett.* **61**, 2526 (1988); A. Dobado, M.J. Herrero, and T.N. Truong, *Phys. Lett. B* **235**, 134 (1990); A. Dobado and J.R. Peláez, *Phys. Rev. D* **47**, 4883 (1993); **56**, 3057 (1997); J.A. Oller, E. Oset, and J.R. Peláez, *Phys. Rev. Lett.* **80**, 3452 (1998); *Phys. Rev. D* **59**, 074001 (1999); **60**, 099906 (1999); F. Guerrero and J.A. Oller, *Nucl. Phys. B* **537**, 459 (1999); A. Dobado and J.R. Peláez, *Phys. Rev. D* **65**, 077502 (2002).
- [11] A. Denner, S. Dittmaier, and T. Hahn, *Phys. Rev. D* **56**, 117 (1997); A. Denner and T. Hahn, *Nucl. Phys. B* **525**, 27 (1998).
- [12] S. Dawson and S. Willenbrock, *Phys. Rev. D* **40**, 2880 (1989).
- [13] S.N. Gupta, J.M. Johnson, and W.W. Repko, *Phys. Rev. D* **48**, 2083 (1993).
- [14] T. Corbett, O.J.P. Eboli, J. Gonzalez-Fraile, and M.C. Gonzalez-Garcia, *Phys. Rev. Lett.* **111**, 011801 (2013); G. Aad *et al.* (ATLAS Collaboration), *Phys. Rev. D* **87**, 112001 (2013); *Eur. Phys. J. C* **72**, 2173 (2012); *Phys. Rev. D* **87**, 112003 (2013); S. Chatrchyan *et al.* (CMS Collaboration), *Eur. Phys. J. C* **73**, 2283 (2013).